Film formation of crystallizable polymers on microheterogeneous surfaces

2005 J. Phys.: Condens. Matter 17 S623

(http://iopscience.iop.org/0953-8984/17/9/020)

INSTITUTE OF PHYSICS PUBLISHING JOURNAL OF PHYSICS: CONDENSED MATTER

J. Phys.: Condens. Matter **17** (2005) S623–S635 doi:10.1088/0953-8984/17/9/020

Film formation of crystallizable polymers on microheterogeneous surfaces

Evelyn Meyer and Hans-Georg Braun[1]

Max-Bergmann Center of Biomaterials Dresden and Institute of Polymers Dresden, D-01069 Dresden, Hohe Straße 6, Germany

E-mail: Meyer@ipfdd.de and Braun@ipfdd.de

Received 24 November 2004
Published 18 February 2005
Online at stacks.iop.org/JPhysCM/17/S623

Abstract

Dewetting and crystallization of thin polyethyleneoxide (PEO) films obtained by dip-coating on microheterogeneous surfaces are investigated. Formation of thin polymer films and crystallization are characterized as sequential processes. Film topography and morphology are influenced by surface pattern geometry and polymer solution properties. Under appropriate experimental conditions in which heterogeneous nucleation is avoided, ultrathin non-crystalline PEO films can be prepared which are stable with respect to crystallization over a long time. The experimental procedure established generates films by *dewetting on microheterogenous surfaces* in which isolated amorphous micrometre-sized areas surrounded from non-wetting barriers are formed. Within these amorphous PEO areas, crystallization can be initiated on request with respect to starting time and location. The crystallization in ultrathin PEO films results in highly branched lamella morphology arising from a diffusion limited aggregation processes (DLA). As time and location for onset of diffusion limited crystallization can be chosen, the morphological features characteristic for DLA growth processes such as correlation width and growth direction of branches can be tuned. In addition, influences of limited material reservoirs in confined areas on film morphology are discussed.

(Some figures in this article are in colour only in the electronic version)

1. Introduction

The principles of organization of ultrathin polymer films in contact with a *microheterogeneous surface* are of great interest for the fundamental understanding of phenomena that determine the structure formation on surfaces as well as the aspect of surface engineering which allows us to direct structural features on predefined locations. Key processes in context with film

[1] Author to whom any correspondence should be addressed.

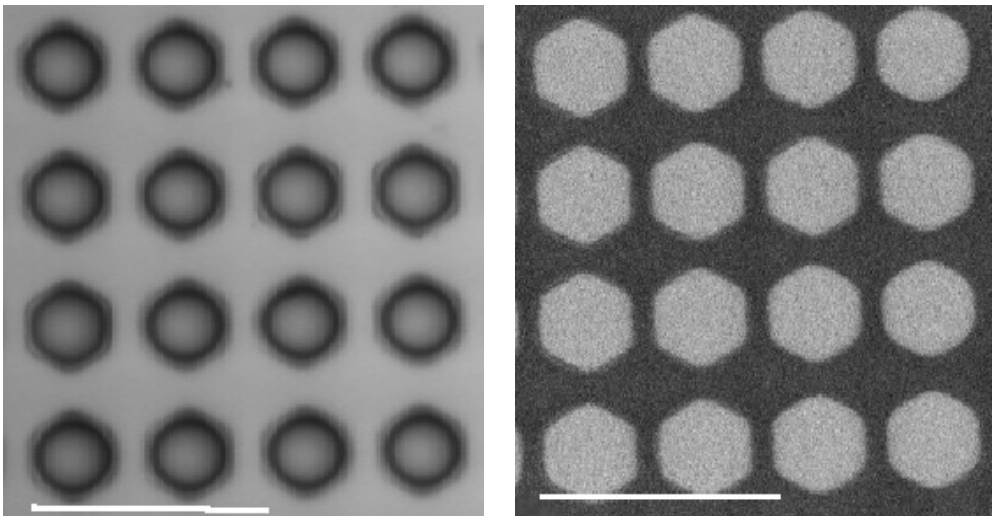

(a) (b)

Figure 1. (a) *Wetting* of water on hydrophilic hexagons. (b) *Dewetting* of hydrophobic polystyrene from hydrophilic hexagons (scale bar: 40 μm).

formation of crystallizable polymers on heterogeneous surfaces are both wetting/dewetting and crystallization processes and their interplay with regard to complex structure evolution. Most of the experimental studies concerning kinetic and morphological aspects of dewetting in ultrathin polymer films were done on *non-crystallizable polymers*. This paper will focus on the study of morphology of *crystallizable* polymers in ultrathin films on microheterogeneous surfaces including peculiarities of crystal growth processes in confined areas.

Depending on the molecular interaction between macromolecules and the underlying surface, ultrathin polymer films may be generated as homogeneous thin films without recognizable defects or they may show morphological features typical for the dewetting scenario including holes, rims etc. As extensively described in the literature dewetting processes can occur due to thickness fluctuations (spinodal type) [1–5] or arise from heterogeneous nucleation [6], whereby the growth of individual holes is initiated from surface defects. As dewetting is a consequence of molecular interactions at the solid/liquid interface the engineering of microheterogeneous surfaces offers an elegant route to control both wetting figure 1(a) [7–9] and dewetting figure 1(b) processes [10, 11]. The microheterogenity of the surface arises from local differences in surface chemical composition. Common methods to achieve surface patterning on various scales are microcontact printing (50 μm–50 nm) [12], electron beam lithography (50 μm–10 nm) [13] or dip-pen writing (50–30 nm) [14]. In all of these methods the heterogenity results from different molecular units in a self-assembled monolayer [15] which bind to substrates such as evaporated gold layers, silicon oxide or aluminium oxide layers.

Beside the chemical heterogenization the corrugation of chemically homogeneous surfaces has also been shown to trigger the dewetting process of thin films [16]. The control of dewetting structures by conformal contact with topographically structured surfaces has recently been investigated by Lee [17].

Appropriate parameters concerning geometrical features of motifs (size, shape and arrangements of motif elements) and of polymer properties (viscosity, concentration, etc) have

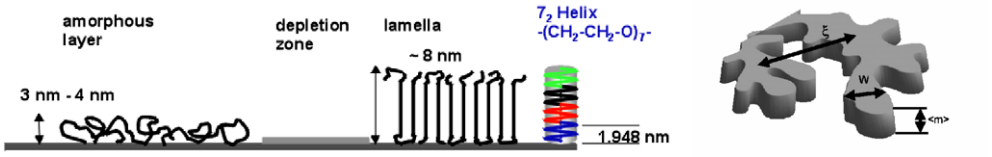

(a) (b)

Figure 2. (a) Basic structural units involved in the crystallization process. Crystalline lamellae are composed of typically four unit cells in which PEO segments are arranged in a 7_2-helical conformation of 1.948 nm basic length. (b) Characteristic features of *DBM* morphologies according to the model of Sommer.

to be chosen in order to guarantee the entirely replication of surface patterns into the film. For striped surface patterns Sharma [18] predicted conditions for correct templating of the surface pattern into a dewetting pattern of the film in terms of film thickness, periodicity and width of the striations defining the surface heterogenity. Ideal templating requires a periodicity interval which is greater than or equal to the characteristic length scale of the dewetting instability (capillary wavelength). Further predictions concerning the evolution of dewetting structures on periodically striped heterogeneous surface patterns with respect to size and periodicity have been published by various authors [19–21].

As already demonstrated for patterned amorphous films the dewetted films show a topography (film thickness variation) dependent on the predefined surface pattern [11]. In the case of crystallizable polymers the film thickness is known to influence the crystallization kinetics. For thin films (30 nm $<$ thickness $<$ 100 nm) it has been found that the spherulitic growth rate is decreasing with increasing film thickness [22–24]. The growth rate change should influence morphological features of crystallized films. Crystallization in ultrathin films results in *densely branched lamellae morphologies* (DBM) which originate from a *diffusion limited aggregation* process (DLA).

Recently Sommer and Reiter [25–27] proposed a molecular model describing the diffusion controlled crystallization process in ultrathin PEO films. Since this model will be essential for the understanding of our experimental findings it will be briefly outlined in figure 2: after nucleation, macromolecules from the initially amorphous layer attach to the crystalline lamella. During this process, the surface area occupied per molecular unit decreases and consequently a depletion zone in front of the lamella appears. This zone has to be overcome by a molecular diffusion process. The key parameters for the quantitative description of the branched morphology are

- the correlation length ξ which describes the average distance between adjacent branches,
- the correlation width w which describes the width of the branch and which is essentially related to the tip radius in other approaches and
- $\langle m \rangle$, which is the height of the morphological unit, which is the lamella thickness in polymer crystals.

Within this model, the thickness differences between the amorphous layer and the crystalline lamella which reflects the surface density jump influence the correlation length. An increase in the surface density jump during crystallization causes an increase in the correlation length. While an increase in crystallization temperature causes an increase in the correlation width of the branch the correlation length is not affected by temperature changes. DBM structures in ultrathin PEO films or interfacial layers have been observed as morphological features

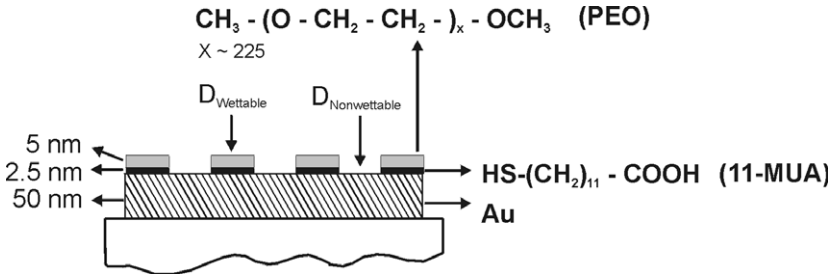

Figure 3. Design of micropatterned surfaces. The hydrophilic carboxy-groups of 11-MUA form areas of preferred wettability for hydrophilic PEO or water. Patterning is achieved by electron-beam or soft lithography.

appearing during crystallization around micropatterned PEO dots [28] or as lamella structures grown in interfacial layers from PEO/PMMA blends accompanied by phase separation [29, 30].

The flexible PEO polymer chains crystallize in an orthorhombic structure with a 7_2-helical chain conformation in the lamellae crystals [31]. The periodicity along the chain axis is 1.94 nm.

In order to influence the crystal growth rate, respectively morphology features, it is a challenge to find conditions which allow us to initiate crystallization processes on request with respect to time and location and to find appropriate geometrical features to direct diffusion controlled growth processes and therefore the texture of crystalline films.

2. Experimental details

2.1. Preparation of micro-patterned substrates

The general surface design is depicted schematically in figure 3. The smooth surface of a cleaned microscopic cover glass or silicon wafer with a 3 nm natural oxide layer is coated with a 2–3 nm chromium layer as adhesion promoter followed by a 50 nm gold layer.

For cleaning, substrates are rinsed with absolute ethanol, distilled water and finally treated in a plasma cleaner (Harrick). Evaporation of chromium or gold was done in a high vacuum coating unit (Leybold Univex 300) equipped with two thermal evaporators. Metal evaporation was performed at a chamber vacuum of 10^{-5} mbar and with typical evaporation rates of 1.0 nm s^{-1}. Surface heterogenization into hydrophilic and hydrophobic domains is achieved by *soft lithography* [12] or *electron-beam lithography* [32]. Depending on the micro-structuring method the patterning of the surface is done as follows.

- By micro-contact printing 11-mercaptoundecanoic acid (11-MUA) molecules are transferred from a flexible polydimethylsiloxane (PDMS) stamp to the gold surface (Au). The remaining unprinted areas are hydrophobized by chemisorption from a 10^{-3} molar octadecylmercaptane (ODM)/ethanol solution.
- For electron-beam lithography the gold surface is modified by chemisorption of 11-mercaptoundecanoic acid from a 10^{-3} molar alcoholic solution. The hydrophilic surface areas exposed to the electron beam become hydrophobic due to molecular changes (most probably through loss of CO_2 from the terminating carboxy groups and cross-linking of the aliphatic hydrocarbons). Typical electron doses required for modification of wettability are 1000 μAs cm^{-2}.

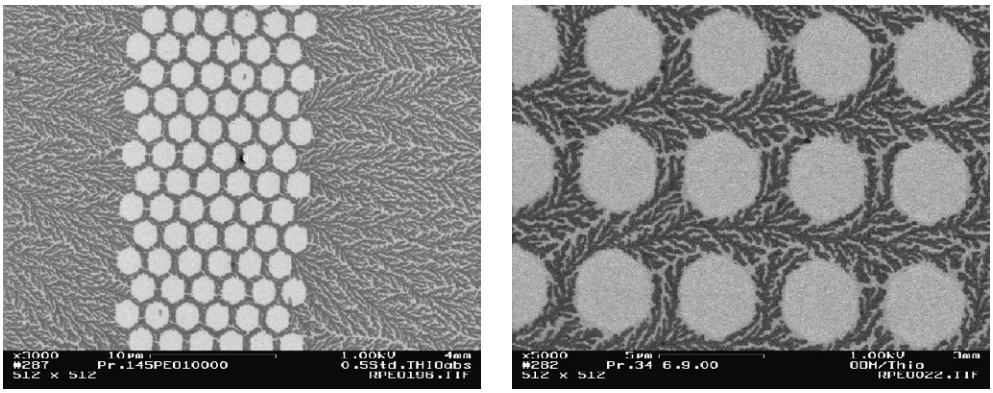

(a) (b)

Figure 4. ((a), (b)) Micropatterned crystalline PEO films; branching of crystalline lamellae due to the *diffusion limited aggregation (DLA)* process within the ultrathin polymer films after dewetting from the microheterogeneous substrate surface.

2.2. Polyethyleneoxide (PEO) film preparation by dip-coating

Ultrathin structured polymer films were prepared by dip-coating of micropatterned substrates from chloroformeous PEO solutions (concentration 0.15% by weight). Hydrophilic areas favour the wetting of hydrophilic PEO [10]. Generally, PEO with a molecular weight M_w 10 000 was used. For experiments concerning the influence of molecular weight on the dewetting morphologies PEO of M_w 6000 and 2000 was taken. The polymers were obtained either from Fluka or Polymer Standards (PSS Mainz). The lift-off velocity of the substrate during dip-coating was typically 2 mm s^{-1}.

2.3. Morphological characterization and instrumentation

The film morphology was characterized by scanning electron microscopy (SEM Gemini DSM 982, LEO Company Oberkochen) typically operating with electron energies of 1 keV down to 500 eV. The low voltage operation favours imaging of thin and ultrathin organic layers (low penetration depth of low energy electrons) and avoids charging of non-conducting surfaces without additional metal coating. For AFM investigations a scanner (*Ultraobjective*®, SIS Company) integrated into a reflective light microscope combined with a dark field mode was used. Dark field imaging was extremely helpful for the detection of ultrathin crystalline structures separated from amorphous metastable film areas. The combination of light microscopic techniques with the AFM adjusted to the light microscope view field allows a pre-selection of metastable amorphous films by optical inspection and a consecutive nucleation by contact with the AFM tip within 2 μm accuracy.

3. Results

3.1. Dewetting versus crystallization

In order to study the crystal morphology of films on heterogeneous surfaces the question of to what extent the dewetting influences the crystallization process is of interest. Microscopic investigations of hydrophilic PEO films on patterned surfaces with μm-sized hydrophobic hexagons show that the PEO solution is clearly removed from the non-wettable hexagons

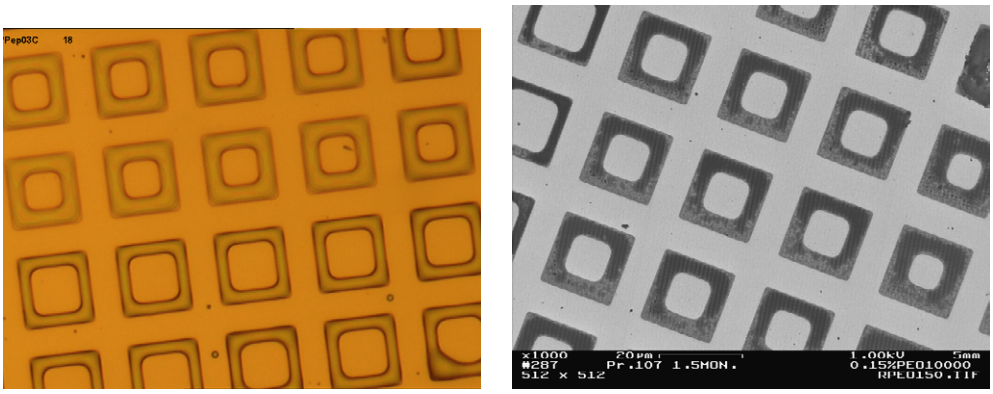

(a) (b)

Figure 5. Topography of (a) liquid layer and (b) solid film.

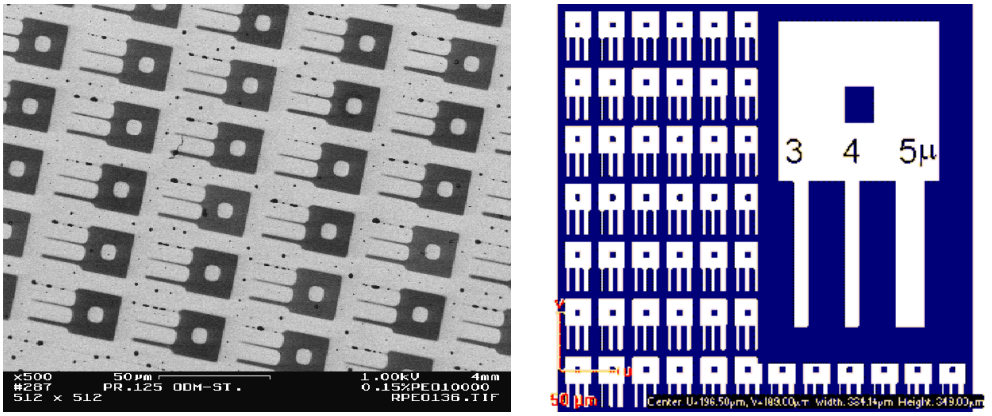

(a) (b)

Figure 6. (a) Imperfect replication of wettable pattern shown in (b); generation of sub-μm droplets on small wettable lines (3 μm) due to Rayleigh instability of PEO solution.

before solidification. The films are initially amorphous immediately after the dip-coating process and after only a short time the heterogenous crystallization begins. The propagation of the crystal growth front can be observed in the dark field mode of a reflection light microscope. The growth velocity at room temperature (23 °C) is about 5.5 μm s^{-1}. The branched lamella growth fronts follow the geometrical features as determined by the surface wettability pattern (figures 4(a), (b)).

The experiments demonstrate that dewetting and crystallization are temporally separated processes. Nevertheless, dewetting influences the film formation because morphological features are determined by the arising topography of the liquid phase during the dip-coating process which depends on the geometry of the surface pattern and the polymer properties. During the dip-coating process the *polymer solution* dewets from the hydrophobic motifs and is transferred onto the hydrophilic areas. The topography of the liquid phase (figure 5(a)) on these wettable areas is replicated in the solid film (figure 5(b)) if the liquid phase is stable during the evaporation process. The influence of 2D-surface pattern geometry on topography and stability of the confined liquid phase been extensively studied by Lipowsky [7].

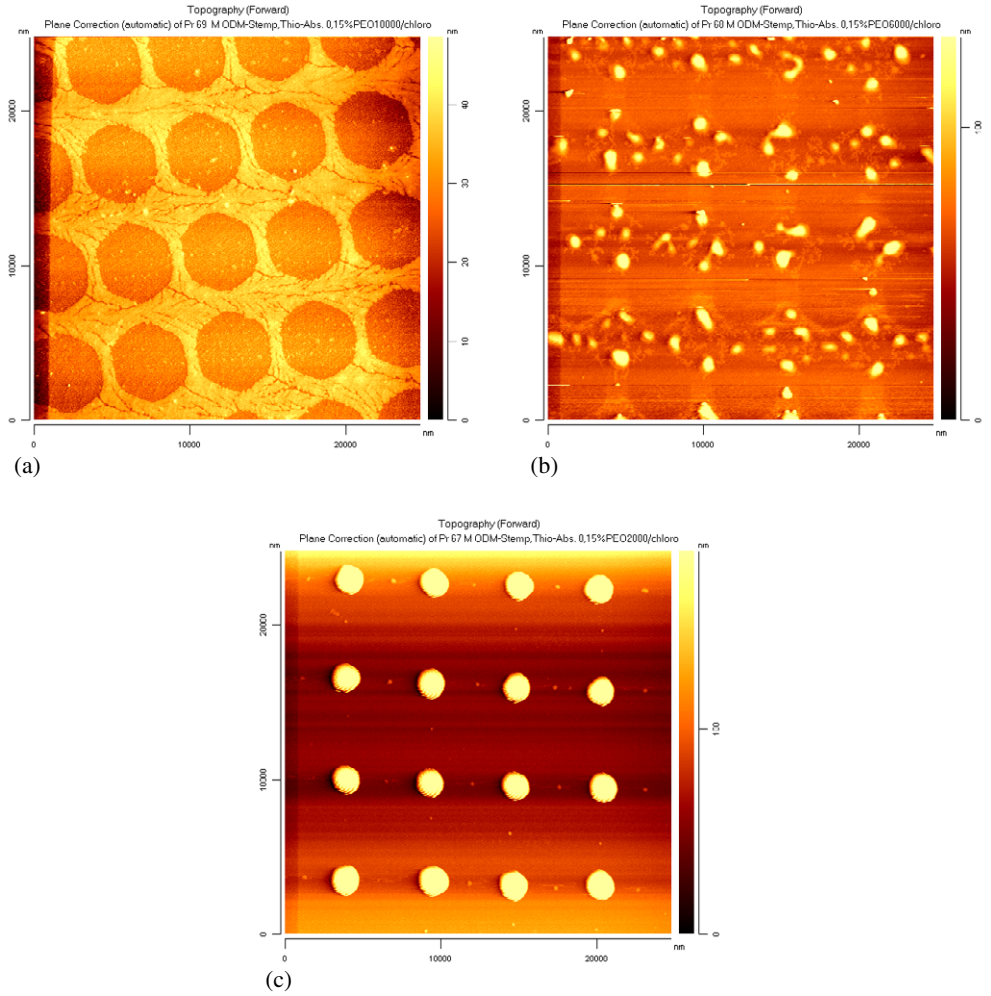

Figure 7. Imperfect replication of the pattern into the film caused by disintegration of the PEO solution during the dewetting process. The stage of disintegration depends on the polymer viscosity (molecular weight). (a) M_w 10 000, (b) M_w 6000, (c) M_w 2000.

An example for imperfect replication of a surface pattern into a film is shown in figure 6(a). The corresponding surface pattern is schemed in figure 6(b). The width of the wettable channel segments decreases from 5 to 3 μm. While the widest striations are completely covered by the PEO film the smallest lines are decorated by a series of small PEO dots which originate from a Rayleigh instability [33] of the liquid PEO solution prior to solidification. The Rayleigh instabilities of a thin liquid film in contact with striped surfaces of wettable and non-wettable motifs have been theoretically predicted by Sharma [18].

The perfect replication of the surface pattern into the film is also dependent on the viscosity of the polymer solution. Figures 7(a)–(c) demonstrate the results of the dip-coating process from PEO of different molecular weight (different viscosity) at the same concentration, on the same micro-pattern and lift-off velocities. The sample with highest viscosity shows a continuous crystalline film on the hydrophilic network which reflects the perfect replication of the predefined hexagon surface pattern (figure 7(a)). Low viscosity causes a rupture of the liquid

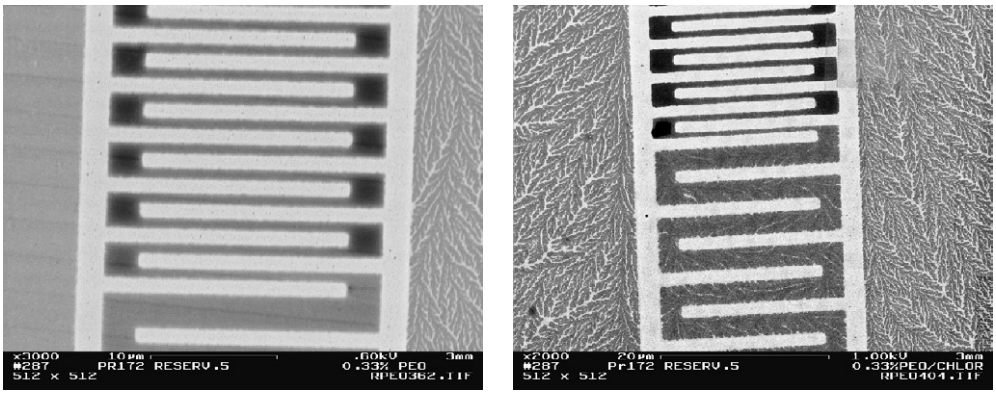

(a) (b)

Figure 8. Variation of crystalline morphology due to film thickness variation by choice of pattern with appropriate proportion of wettable and non-wettable areas.

phase prior to polymer solidification and results in the formation of solidified PEO droplets (figure 7(c)). These are finally centred within the *nodal points* between the non-wettable hexagonal motifs. Decreasing polymer concentration causes formation of smaller dots. This procedure allows the preparation of regular spaced submicrometre polymer dots. Figure 7(b) shows an intermediate state of the disintegration of the polymer solution corresponding to an intermediate viscosity.

Lamella growth features can also be controlled by the geometry of the pattern. Appropriate choice of proportion of wettable and non-wettable areas in the motifs causes different thicknesses of the liquid phase during the dewetting process which lead to different morphological features in the solid film. Whereas ultrathin films crystallize in branched lamellar structures thicker areas grow in compact non-branched PEO lamellae (figure 8).

3.2. The initial state of PEO as dewetted

In our experiments we observed that *small* μm*-sized isolated areas of PEO*, like the droplets shown in figure 9(a), are stable in the amorphous state for a long time. The shape of these solidified PEO droplets can be fitted by a spherical cap function [34] (figure 9(c)) as typically used to calculate liquid droplet shapes.

Crystallization of the droplets can be initiated by contact with an AFM tip. Due to the crystallization, the initially spherical shaped drop is changed to a single- or multi-lamella stack as shown in figures 9(b) and (d).

The observation that small *isolated* PEO droplets are obviously amorphous for a long time leads to the experiment to create geometrically defined isolated PEO film segments by dewetting on appropriate heterogenized surfaces. Micrometre-sized hydrophilic areas are isolated by typically 1–2 μm sized hydrophobic barriers which are realized by electron beam lithography of the self-assembled monolayers of hydrophilic 11-MUA molecules. Figures 10(a) and (b) demonstrate the amorphous state inside the isles whereas outside the barriers crystalline structures are already formed. The reason for the stability of the amorphous segment inside the rings is the low probability finding a nucleation site in micrometre-sized areas. Consequently, the heterogeneous nucleation is avoided.

Surface heterogenization by the electron beam allows the preparation of more complex geometries as shown in figure 11(a). The possibility

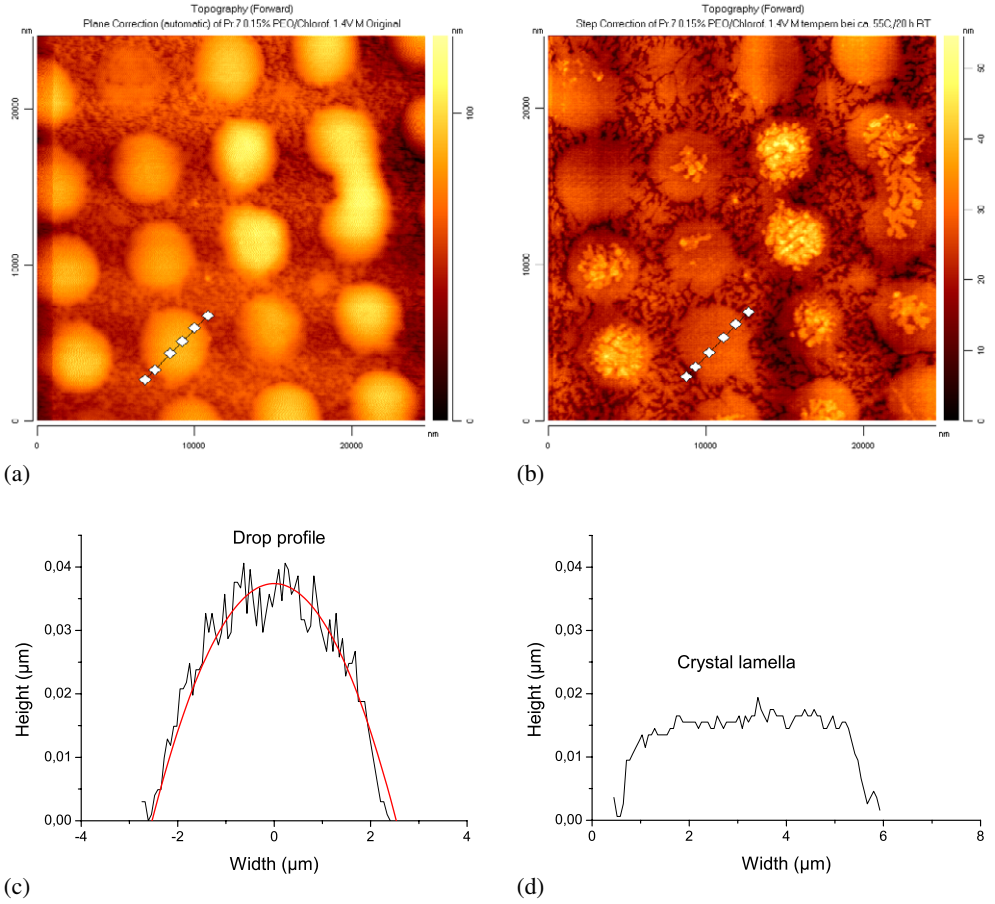

Figure 9. AFM micrographs of (a) dewetted and (b) crystallized PEO morphologies and corresponding height profiles of the amorphous (c) and crystallized droplets (d). A spherical cap fit of the raw data in (c) yields the height of the droplet as 0.037 μm, the radius as 2.50 μm and the included volume as 0.363 μm^3. Within the experimental error the volume of the droplet is equivalent to the volume of the crystal lamella but the radius of the crystallized structure is increased.

- to prepare longtime metastable amorphous PEO film segments in isolated areas and
- to initiate the crystallization by the AFM tip

offers a unique chance to control crystal growth processes with respect to *starting time*, *starting location* and *growth direction*. Figure 11(b) shows the same area as in figure 11(a) but after nucleation by external stresses released through contact with a AFM tip. The nucleation site and direction of the growth front are clearly recognizable.

The nucleation process can not only be controlled by external stresses but also by surface topographical effects. Surface scratches or surface steps represent nucleation centres as shown in figures 12(a) and (b). The dendritic growth front propagates perpendicular to the nucleating line structures. The surface topography is an additional feature to control the DLA growth morphologies. It should be noted that surface topographies which act as nucleating lines can also arise from dewetting structures of the polymer itself. In particular, rims are starting points for crystallization.

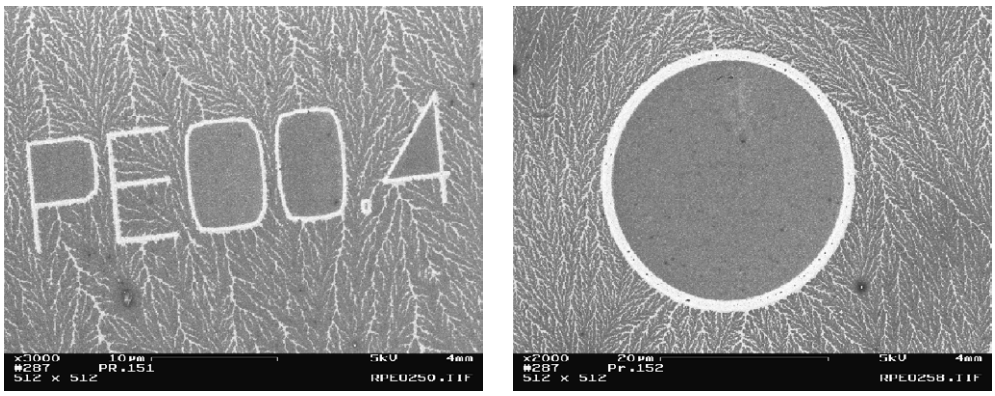

(a) (b)

Figure 10. Amorphous PEO areas separated from crystallized continuous film by a hydrophobic barrier.

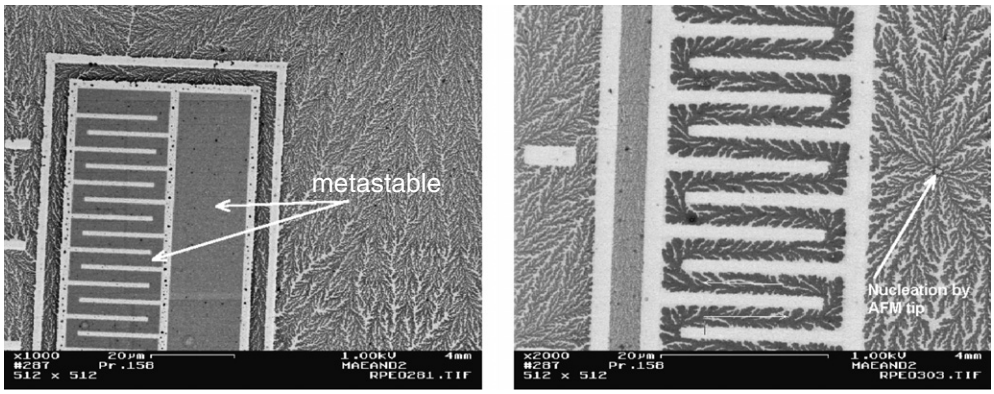

(a) (b)

Figure 11. Isolated amorphous PEO areas (a) are nucleated by contact with an AFM tip (b). The radial growth of branched lamellae follows the predefined structure given by the channel geometry.

3.3. Influence of temperature and geometrical confinement on morphological features

The ability to prepare long time stable amorphous films which can crystallize on request offers the opportunity to control morphological features as a function of temperature. Figure 13 shows a sequence of SEM images with crystalline morphologies grown at different temperatures. The nucleation was initiated approximately in the centre of each circle. The growth history can be easily reconstructed from the direction of the branches which are oriented towards the lamella growth front.

The observed branched lamella morphologies will be discussed within the theoretical approach that has been established by Sommer and which has been sketched out in the introduction. The typical branching structures result from non-equilibrium growth processes in which disordered PEO chains diffuse from an ultrathin amorphous film to a crystalline lamella.

The initial thickness of the amorphous film in the temperature dependent crystallization experiments was 4 nm as determined by ellipsometry. The thickness of crystalline lamellae varies with temperature from about 8 nm to about 25 nm or more. Crystallization experiments

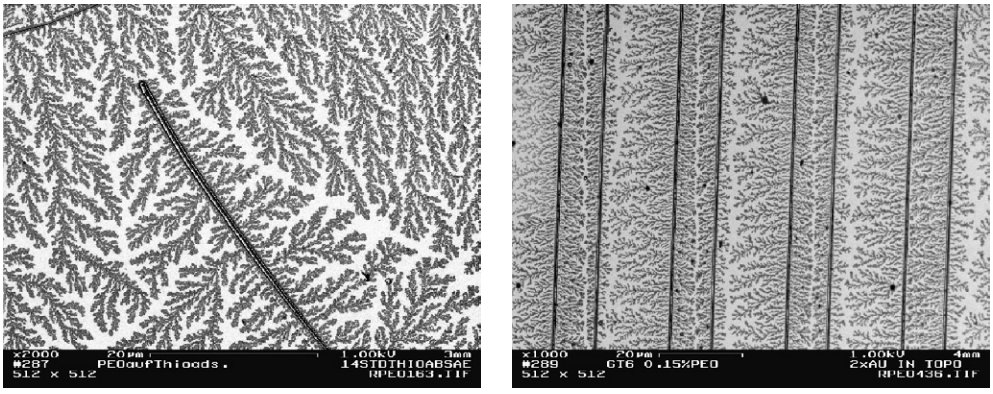

(a) (b)

Figure 12. Topographically induced lamella growth fronts originating (a) from a surface scratch and (b) from a defined topographical step pattern.

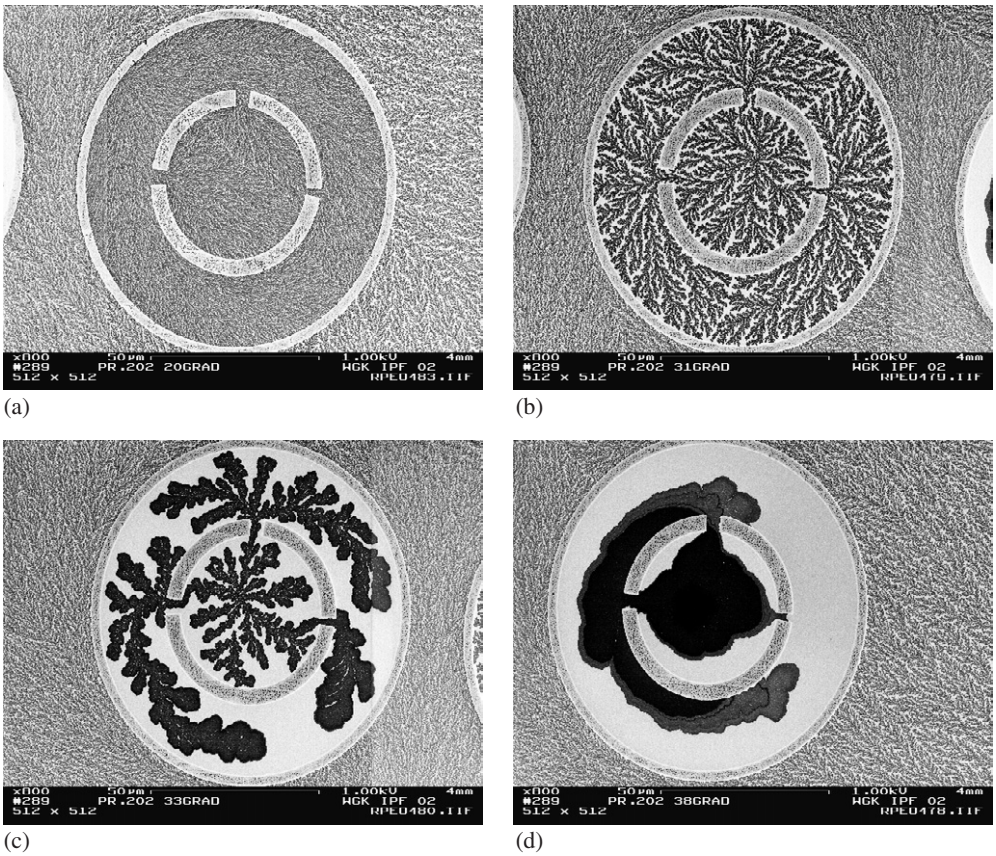

(a) (b)

(c) (d)

Figure 13. (a) 21 °C, (b) 31 °C, (c) 33 °C, (d) 38 °C.

at 20 °C (high undercooling) as shown in figure 13(a) result in a fine branched unilamella structure of 8 nm thickness. Increasing crystallization temperatures lead to branch growth with larger tip radius or correlation width. Higher temperatures favour molecular reorganization

processes which drive the system towards thermodynamic equilibrium. This causes a larger correlation width respectively tip radius of branches. Figure 13(c) clearly reveals that morphological features of branches are changed with progressive growth despite isothermal growth conditions. The tip radii increase and the growth velocity has been found to decrease. Additionally, the thickness of the lamella is increasing which indicates that the chains become more extended and approach the thermodynamic equilibrium state. Branches growing from opposite sites in the confining channels cannot contact each other due to very large depletion zones at the growth front. Due to the limited material reservoir in confined structures growth kinetics and consequently growth morphology are changed. The scenario on the molecular level is as follows: for a lamella branch growing inside the confinement the width of the depletion zone is continuously increased due to the geometrical constraints and therefore the concentration gradient at the growth front is decreased. This reduces the number of molecules/time which attach to the lamella front. As newly approaching molecules at the interface can impede reorganization processes a decreasing number of attaching molecules favours structural reorganization closer the equilibrium morphologies. A further increase in crystallization temperature as seen in figure 13(d) causes a nearly complete loss of branches and results in multi-lamella stacked structures of up to 25 nm total thickness.

4. Summary

In ultrathin PEO films dewetting and crystallization are temporarily separated processes. However, dewetting determines the topography of initially amorphous PEO films which depends on pattern geometry and polymer properties and therefore crystalline morphological features such as lamella thickness and lamella branching. In PEO films the crystallization process is initiated by heterogeneous nucleation. Film formation on isolated μm-sized areas creates long time stable amorphous film segments which can be crystallized on request with respect to starting time and location. The crystallization can be initiated by contact with a AFM tip. This procedure allows us to control morphological features in dependence on temperature, pattern geometry etc. In ultrathin films crystallization results in highly branched structures which can be described theoretically by a modified model of the diffusion limited aggregation process. In confined geometries structural features are modified during isothermal growth processes by change of the growth kinetics due to the limited material reservoir.

Acknowledgment

The authors wish to thank the *Deutsche Forschungsgemeinschaft* for financial support within the priority programme *Wetting and structure formation at surfaces*.

References

[1] Seemann R, Herminghaus S and Jacobs K 2001 *Phys. Rev. Lett.* **86** 5534
[2] Thiele U, Mertig M and Pompe W 1998 *Phys. Rev. Lett.* **80** 2869
[3] Reiter G 1992 *Phys. Rev. Lett.* **68** 1992
[4] Ruckenstein E and Jain R K 1974 *Faraday Trans.* II **70** 132
[5] Sharma A and Reiter G 1996 *J. Colloid Interface Sci.* **178** 383
[6] Jacobs K, Herminghaus S and Mecke K R 1998 *Langmuir* **14** 965–9
[7] Lipowsky R 2001 *Curr. Opin. Colloid Interface Sci.* **6** 40
[8] Brinkmann M and Lipowsky R 2003 *J. Appl. Phys.* **92** 4296
[9] Gau H, Herminghaus S, Lenz P and Lipowsky R 1999 *Science* **283** 46–9
[10] Meyer E and Braun H G 2000 *Macromol. Mater. Eng.* A **276/277** 44–50
[11] Braun H G and Meyer E 1999 *Thin Solid Films* **345** 222–8

[12] Xia Y and Whitesides G M 1998 *Angew. Chem. Int. Edn Engl.* **37** 550–75
[13] Harnett C K, Satyalakshmi K M and Craighead H G 2000 *Appl. Phys. Lett.* **76** 2466
[14] Piner R D, Zhu J, Hong S and Mirkin C A 1999 *Science* **283** 661–3
[15] Ulman A 1991 *Ultrathin Organic Films: from Langmuir–Blodgett to Self-Assembly* (Boston, MA: Academic)
[16] Rehse N, Wang C, Hummel M, Georgejahn M, Magerle R and Krausch G 2001 *Eur. Phys. J.* **4** 69–76
[17] Suh K Y, Park J and Lee H H 2002 *J. Chem. Phys.* **116** 7714–8
[18] Kargupta K and Sharma A 2001 *Phys. Rev. Lett.* **86** 4536–9
[19] Bauer C and Dietrich S 1999 *Phys. Rev.* E **60** 6919–41
[20] Thiele U, Brusch L, Bestehorn M and Baer M 2003 *Eur. Phys. J.* E **11** 255–71
[21] Sehgal A, Ferreiro V, Douglas J F, Amis E J and Karim A 2002 *Langmuir* **18** 7041–8
[22] Massa M V, Dalnoki-Veress K and Forrest J A 2003 *Eur. Phys. J.* E **11** 191–8
[23] Despotoupolou M M, Frank C W, Miller R D and Rabolt J F 1996 *Macromolecules* **29** 5797
[24] Frank C W, Rao V, Despotoupolou M M, Peace R F W, Hinsberg W D, Miller R D and Rabolt J F 1996 *Science* **273** 4536
[25] Reiter G and Sommer J U 1998 *Phys. Rev. Lett.* **80** 3771
[26] Reiter G and Sommer J U 2000 *J. Chem. Phys.* **112** 4376–83
[27] Sommer J U and Reiter G 2000 *J. Chem. Phys.* **112** 4384
[28] Wang M, Braun H-G and Meyer E 2002 *Macromol. Chem. Rap. Commun.* **23** 853–8
[29] Wang M, Braun H-G and Meyer E 2003 *Polymer* **44** 5015
[30] Wang M, Braun H-G and Meyer E 2004 *Macromolecules* **37** 437
[31] Takahashi Y and Tadokoro H 1973 *Macromolecules* **6** 672
[32] Harnett C K, Satyalaksmi K M and Craighead H G 2001 *Langmuir* **17** 178–82
[33] Rayleigh 1879 *Proc. R. Soc.* **29** 71–97
[34] Erbil H Y 1998 *J. Phys. Chem.* B **102** 1964